REAL-TIME RADIO FREQUENCY INTERFERENCE DETECTION AND MITIGATION WITH THE FRONT-END GNSS INTERFERENCE EXCISOR (FENIX)

J. Querol[*]

University of Luxembourg
Interdisciplinary Centre for
Security, Reliability and Trust (SnT)
29, Avenue John F. Kennedy
L-1855 Luxembourg, Luxembourg

A. Perez, J.F. Munoz-Martin, A. Camps[†]

Universitat Politècnica de Catalunya/IEEC,
Signal Theory and Communications Dept.
Unidad María de Maeztu - CommSensLab
C/ Jordi Girona 1-3, D4 building
08034 Barcelona, Spain

ABSTRACT

The number of applications based on Global Navigation Satellite Systems (GNSS) has been increasing in the last years. With its proliferation, Radio-Frequency Interference (RFI) has become one of the most concerning topics on GNSS-based devices for navigation, positioning and timing, but also for Earth Observation purposes such as GNSS-Reflectometry (GNSS-R) and GNSS-Radio Occultations (GNSS-RO) due to the corruption of the received signal and the corresponding geophysical measurements. The Front-End GNSS Interference eXcisor (FENIX) mitigates the problem of RFI by providing a plug-and-play solution which, placed between the antenna and the receiver, excises virtually any kind of interference signal, as its mitigation algorithm is agnostic on the particular type of RFI. The new version of FENIX is also capable of operating with large signal bandwidths (∼50 MHz) and dual-band applications (e.g. L1 + L2 or L1/E1 + L5/E5). This paper shows the performance of the system for commercial GNSS receivers and GNSS-R applications. The use of FENIX in Microwave Radiometers is also possible, but it is out of the scope of this paper.

***Index Terms*—** RFI, detection, mitigation, GNSS, GNSS-R, reflectometry, FENIX, MFT.

1. INTRODUCTION

The main goal of the FENIX is the mitigation of RFI signals that cause desensitization, signal loss, or in general the malfunction of a GNSS receiver. FENIX is a patented technology (US 15222036) designed to mitigate virtually any type of RFI signals regardless of the antenna and the receiver used by the system. It uses a non-parametric algorithm based on a combination of statistical techniques and the Multiresolution Fourier Transform (MFT), bestowing it with the capability to work against any kind of RFI without prior knowledge of its characteristics. The new FENIX prototype is shown in Fig. 1. Its physical dimensions are 10 cm x 5 cm x 2 cm, it weights 170 g and it is USB powered.

Fig. 1: New portable and standalone FENIX prototype with dimensions 10 cm x 5 cm x 2 cm and USB powered.

In this paper, the new architecture of the FENIX system is presented. It improves the performance and capabilities of prior versions, allowing for improved robustness and flexibility against RFI. First, the FENIX block diagram is presented, including the Radio Frequency (RF) and Signal Processing (SP) stages. Then, results are presented in terms of: 1) the transfer function versus the RFI type and power, showing that the delay is constant, and agnostic to the RFI type and/or power, 2) resilience improvement of GNSS receivers against RFI and finally 3) the application to a GNSS-R receiver.

[*]Thanks to the Signal Processing and Communications (SIGCOM) research group of SnT – University of Luxembourg for funding.

[†]This work was supported by the Spanish Ministry of Economy and Competitiveness, by the Spanish Ministry of Science, Innovation and Universities, "Sensing with Pioneering Opportunistic Techniques", grant RTI2018-099008-B-C21, by the Remote Sensing, Antennas, Microwaves and Superconductivity Group (CommSensLab) - Unidad de Excelencia María de Maeztu MDM-2016-0600, by the ICREA Academia award by the Generalitat de Catalunya, by the project "FENIX - Front-End GNSS Interference eXcisor" PRODUCTE (2016 PROD 00062) of the AGAUR - Generalitat de Catalunya and by the UPC spin-off company MITIC Solutions S.L.

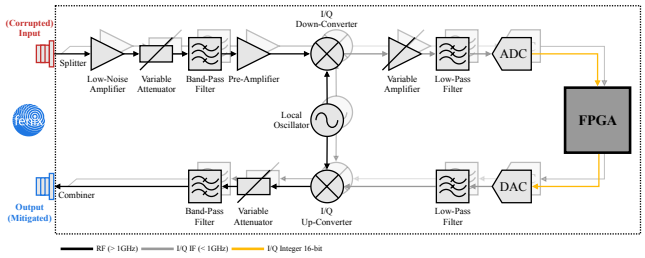

Fig. 2: Block diagram for the RF Stage of the FENIX [1].

2. BLOCK DIAGRAM

The functional block diagram of the system can be divided into two sub-blocks: an analog Radio Frequency (RF) stage and a digital Signal Processing (SP) stage. On one hand, the RF stage amplifies and down-converts the collected signals from the antenna in two separate bands (e.g. L1 + L2 or L1/E1 + L5/E5) and delivers them to the SP stage. Moreover, it takes the RFI-mitigated signals at the output of the SP stage, up-converts them using the same Local Oscillator (LO) and delivers them to the GNSS receiver. On the other hand, the SP stage filters and excises undesired RFI and jamming signals from useful GNSS signals for each of the RF bands independently.

2.1. Radio Frequency Stage

In the RF stage, the signal coming from the antenna (which may be RFI-contaminated or not) is amplified, filtered, down-converted and digitized for subsequent processing in the FPGA. After that, the already processed signal is up-converted to the original frequency band, filtered once again, and attenuated to keep the GNSS receiver out of saturation. This process makes FENIX transparent to the GNSS receiver, thereby providing increased versatility when compared to other RFI detection and mitigation systems. Fig. 2 illustrates a block diagram of the RF stage.

The input signal is first split into two separate paths, each one processing a different frequency band (e.g. L1/L2, L1/L5, etc.). At each branch, the signal is amplified using a Low Noise Amplifier (LNA) to optimize the Noise Factor (NF) of the overall chain. Moreover, GNSS signals captured by the antenna have very low power, on the order of -125 dBm [2], and therefore must be first amplified to adapt their power level to the dynamic margin of the following elements of the chain. On the contrary, if a high-gain GNSS antenna with an integrated LNA is connected to the FENIX, the receiving chain may enter into saturation. To avoid that, a programmable and variable attenuator is placed after the LNA.

After that, two band-pass filters tuned at each center frequency are used. The purpose of these filters is two-fold. On one hand, they reject near-band interference signals, and on the other hand, they avoid saturation and instabilities in the receiving chain. In the same way, the amplifiers are also tuned to allow only the desired frequency band to pass to maximize the near-band rejection. Finally, a pre-amplifier is used after the band-pass filter at each band to adapt the GNSS power level to the down-conversion stage.

At each branch, the analog frequency conversion stage converts the GNSS signals from their band down to an Intermediate Frequency (IF). The down-converted analog signal at IF is transformed into a digital signal using an Analog-to-Digital Converter (ADC). Thus, the digital signal is a representation of the received analog signal coming from the antenna at a lower frequency, filtered and digitized, and it may be RFI-contaminated. Moreover, the signal is usually down-converted using an in-phase and quadrature (I/Q) demodulator, and thus, dual-channel ADCs are used in the digitization process.

Before the digital conversion, the down-converted signals are amplified and filtered again. A variable amplifier is used to adapt the signal power level to the dynamic margin of the ADC, while a low-pass filter prevents aliasing effects, as they may enhance the effects of near-band interference. For this reason, selective low-pass filters are required before digitizing.

The GNSS signals are then digitally processed to detect and eliminate possible RFI signals. The digital signal processing algorithm is implemented in real-time inside an FPGA. The output of the FENIX excision algorithm is connected to a dual-channel Digital-to-Analog Converter (DAC). Then, the RFI-mitigated GNSS signals are converted back to the analog domain from the IF.

Nearing the output, the signals are low-pass filtered again to avoid aliasing, and then up-converted to the original frequency band. The time-lapse between the instants where the signal is down- and up-converted is not zero, and it depends mainly on the delay introduced by the SP stage. However, it is constant and the same for all satellites, and therefore it does not affect the estimation of the navigation solution.

Finally, once the RFI-mitigated GNSS signals are at the original frequency, a variable attenuator is used to avoid saturation at the GNSS receiver. Furthermore, the signals are band-pass filtered again to reduce the coupling of the LO at the output. Finally, the signals from both frequency bands are combined and delivered to the receiver.

2.2. Signal Processing Stage

As mentioned above, the SP stage is completely digital, and it is implemented into an FPGA because of the high throughput required, the large number of logic cells, and pipeline architecture needed to implement the FENIX mitigation algorithm. Fig. 3, thus providing real-time dual-band mitigation.

The signal digitization and quantification at the ADC is performed with 12 bits for each I/Q component. This value ensures a low quantification noise, and a large digital

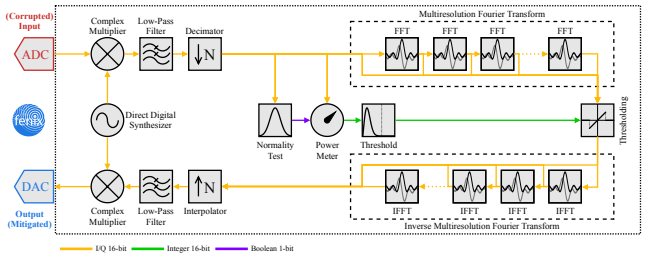

Fig. 3: Block diagram for the SP Stage of the FENIX [1].

dynamic range (∼72 dB). Moreover, a second and digital down-conversion is performed using 16-bit complex multipliers. The digital LO is implemented using a Direct Digital Synthesizer (DDS), which is used for both up- and down-conversion as in the RF stage. This second down-conversion is used to remove the leakage of the analog LO.

Once the signals are at Base-Band (BB), they are low-pass filtered and decimated (only if the signal has been over-sampled at the ADC). This low-pass filter is an FIR filter with a large number of coefficients (>128) to preserve the phase response, to have high selectivity, and, thus, to provide good rejection for near-band RFI signals.

Once the signal has been decimated, two tasks are performed in parallel. In the central branch, a normality test is first applied to the digital data to determine if the incoming samples are RFI-contaminated or not (i.e. if they follow a Normal distribution or not). Thus, the properties of the signal in the statistical domain are first used to take the necessary actions in the RFI mitigation process. The result of the normality test can be obtained as a combination of independent statistical tests such as the complex kurtosis and the Anderson-Darling (A-D) test. In this case, the complex kurtosis is used as a principal normality test, whereas the A-D test can be used as an auxiliary flag to check if the kurtosis is working at its blind spot [3, 4].

If the Normality test determines that the decimated BB samples are Normal, their power (i.e. their variance σ_n^2 for zero-mean signals) is estimated to obtain the threshold value. There are several procedures to estimate the power of the RFI-free samples. The simplest approach consists of using the unbiased sample variance. One of the main drawbacks of this approach is the bias introduced by outliers, which may be likely to appear in RFI environments. A more trustful approach is to use robust estimators such as the Median Absolute Deviation (MAD) or the Inter-Quartile Range (IQR), which provide results less affected by outlier values [5].

Once the variance of the noise has been estimated, the threshold α can be obtained as a function of the desired probability of false alarm, P_{FA}. Suitable values for P_{FA} for GNSS signals are in the range from 10^{-5} to 10^{-6} [1], because of their spread-spectrum correlation gain. The threshold value can be obtained both from the power of the samples (i.e exponential or chi-squared distribution), or equivalently from their root square or absolute value (i.e. Rayleigh or χ distribution). The last option is chosen to keep the samples working at 16-bit integer precision. Therefore, the threshold α can be calculated as

$$\alpha = \sqrt{2}\,\sigma_n \sqrt{ln\left(\frac{1}{P_{FA}}\right)}. \tag{1}$$

Moreover, in the upper branch, the different time-frequency decomposition levels of the BB samples are calculated using the already mentioned MFT algorithm. A set of FFT blocks with different lengths are calculated simultaneously from the BB data. Since they have different transform length, they have different time-frequency resolution. The MFT can be defined as

$$X\left[p,k,r\right] = \frac{1}{\sqrt{r}} \sum_{m=0}^{r-1} x\left[m+pr\right] w_r\left[m\right] e^{-j2\pi\frac{k}{r}m} \tag{2}$$

where $x[m]$ is the input signal, m is the time sample number, $w[m]$ is the transform window (e.g. rectangular, flat-top, Gaussian, etc.), p is the transformed time bin number, k is the frequency bin number, and r is the resolution or scale level.

Therefore, the output of the MFT is a 3-dimensional space wherein the input signal is analyzed in time and frequency domain with different time-frequency resolution levels. Usually, man-made RFI signals have their power concentrated in either time, frequency, or both domain, to maximize the instantaneous and/or spectral power density. This makes the MFT an optimum tool to perform agnostic RFI mitigation. If the MFT is compared with other RFI mitigation techniques in the state-of-the-art, it combines features from both the Short-Time Fourier Transform (STFT) and the Wavelet Transform (WT). The STFT uses the FFT to compute efficiently the spectrum of a signal, whereas the WT changes the length of its transform basis (i.e. mother wavelet) to provide multi-resolution or multi-scale analysis. The MFT provides representation in a 3-dimensional space defined by the domains of time, frequency, and scale. In this way, the RFI signals are projected into different orthogonal spaces with different ratios of time-frequency resolution. The probability of being a version sufficiently similar to the interfering signal received in the base of the transform is maximized to be able to be detected in the subsequent step, once it is compared with the corresponding transformation of the useful signal. The MFT was not previously used to eliminate RFI, and it has been demonstrated to have an overall better behavior than other types of transforms [1].

At the *thresholding* stage, samples with magnitude larger than the threshold α are blanked out. This procedure allows minimizing the Interference-to-Noise Ratio (INR), thus maximizing the SNR because of the properties of the GNSS signals buried into the thermal noise. Therefore, the thresholding excises RFI-contaminated samples from the RFI-free ones. If

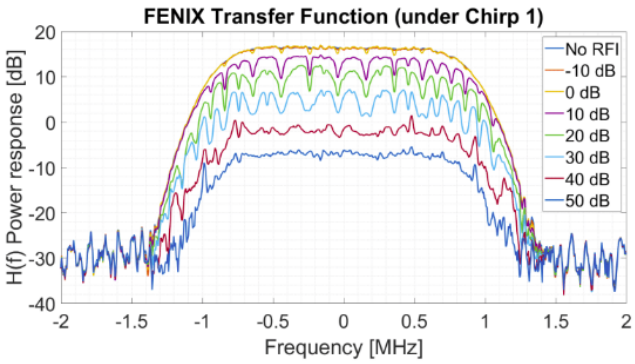

(a) Transfer function with a wideband chirp RFI.

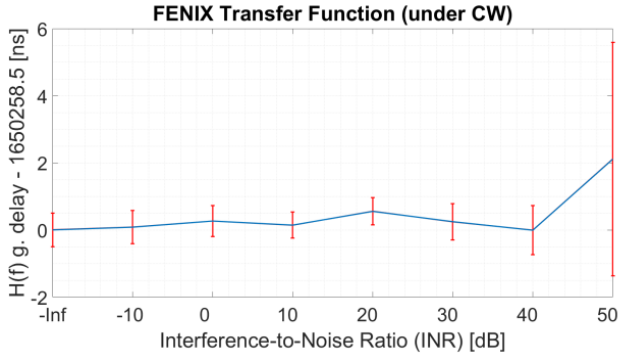

(b) Jitter analysis of the delay introduced by FENIX.

Fig. 4: Sample measurement of the adaptive transfer function of the FENIX. Both magnitude and phase group delay are analyzed [1].

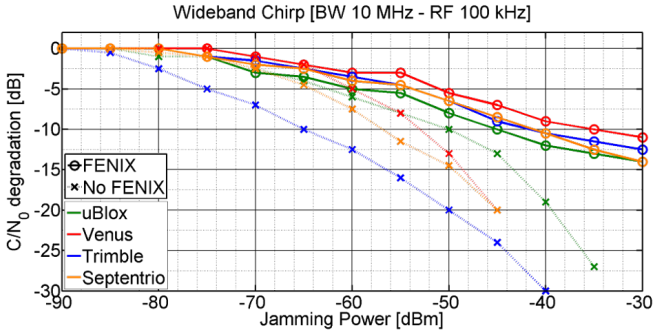

(a) Degradation test for four different GPS Receivers.

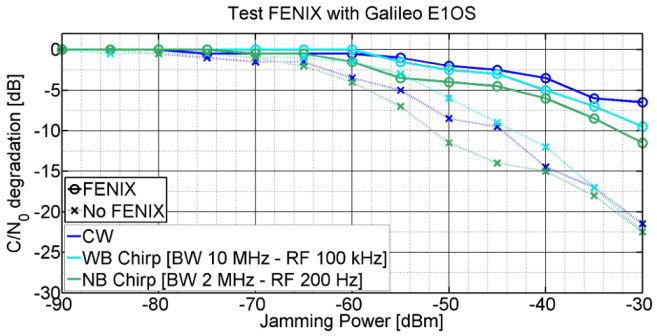

(b) Degradation test with a GALILEO Trimble receiver.

Fig. 5: Multiple C/N_0 degradation tests performed with commercial GNSS receivers. The dotted lines represents systems without FENIX whereas the solid lines correspond to FENIX enabled [1].

each resolution level performs a normalized transform, the same value of α can be applied to all of them. Once the thresholding is applied, the inverse MFT is applied to transform the RFI-mitigated signal samples back to the time domain.

3. PRELIMINARY TESTS

To validate the performance of the new architecture, the FENIX has been tested with COTS GNSS receivers and a GNSS-R system under different RFI scenarios.

3.1. Transfer Function

First of all, the end-to-end transfer function of the new architecture has been calculated. Fig. 4a shows a sample amplitude transfer function for different INR levels. This alone provides much of the information about the performance of this new architecture. The main idea is that the equivalent transfer function to the FENIX adapts itself to excise as much as RFI signal power as possible while it protects the GNSS signal. A different transfer function is obtained if the RFI scenario is changed. Moreover, the delay (i.e. phase derivative of the transfer function) provides an important insight for the analysis of the performance of the FENIX and it is a critical parameter for timing GNSS receivers.

A large but constant delay is introduced by the SP stage. This must be measured so as to calibrate and compensate it in holistic implementations of FENIX with other GNSS Systems. Previous tests for existing FENIX implementations have shown constant delays of about 1.65 ms [1]. As its jitter has been measured to be lower than 2 ns (Fig. 4b), it makes it compatible with 5G applications as they have a Time Alignment Error (TAE) requirements of 65 ns for current 5G Non-Standalone (NSA), 13 ns for next coming 5G Standalone (SA) Sub-6, and 2.6 ns for future 5G mmWave [6, 7]. It is acknowledged that in other more sophisticated applications, such as Galileo reference stations or GNSS timing receivers, the constant delay must be compensated for.

3.2. COTS GNSS Receivers

After the transfer function has been obtained, its performance with different Commercial-Off-The-Shelf (COTS) GNSS receivers is tested. The FENIX system has demonstrated its capability to increase by 20-30 dB [1] the rejection to RFI.

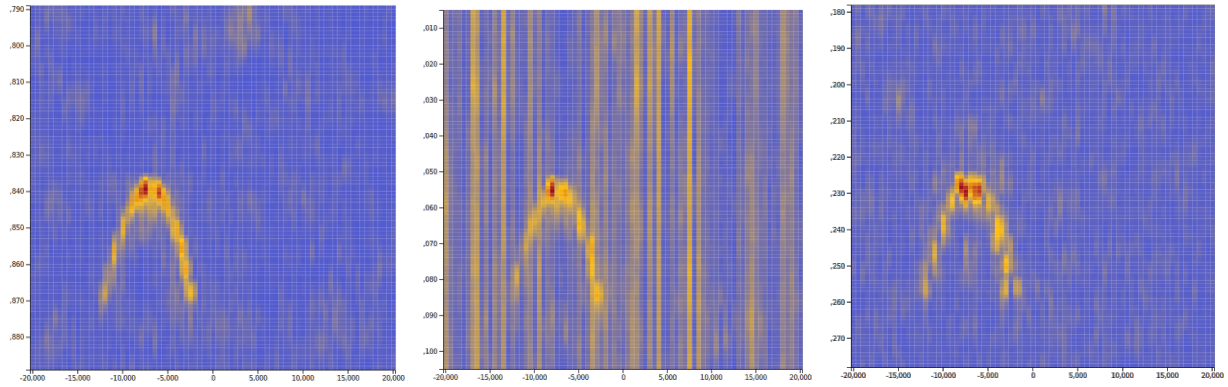

(a) DDM without RFI signal. (b) DDM with a CW RFI. (c) DDM of the mitigated signal.

Fig. 6: Comparison effect of the FENIX performance in GNSS-R observables.

Note that this improvement is compatible with other RFI detection/mitigation techniques at antenna level such as Novatel's GAJT [8], or in post-correlation. Fig. 5 shows multiple C/N_0 degradation tests performed with commercial GNSS receivers. Fig. 5a corresponds to the degradation test for four different GPS receivers with a particular RFI scenario (a wideband chirp signal with 10 MHz od bandwidth and 100 kHz of repetition frequency). Fig. 5b depicts the degradation test with a GALILEO Trimble receiver under three different RFI scenarios.

For GNSS timing applications, the FENIX introduces a constant delay due to the processing stage, but regarding the group delay as a function of the INR, the bias is below the ns level for INR values below 40 dB. However, the standard deviation is a bit larger with a maximum of about 2 ns at 40 dB INR (Fig. 4b). Even though this is the worst-case, the performance in terms of group delay stability remains at ns level. This proves that FENIX can be used even with high precision and high-performance GNSS receivers since the timing accuracy is degraded few ns in the worst case.

3.3. GNSS-R System

Finally, the performance in a GNSS-R case is presented. With the increasing importance of GNSS-based Earth Observation techniques in the last decades, e.g. GNSS-RO and GNSS-R, verifying the improvement of FENIX in these systems is of utmost importance, needless to say in Microwave Radiometers, as it has been shown that getting scientific data from some missions, in some parts of the world turns to be almost mission impossible (e.g. SMOS in some regions of the world [9]).

In GNSS-R, the so-called Delay-Doppler Maps (DDMs) are used to characterize the scattering of the GNSS signals off the Earth's surface by calculating the cross-correlation of the received signal with a locally generated replica of the transmitted one at different time delays and Doppler frequency shifts. Current spaceborne GNSS-R systems use 1 ms coherent integration followed by 1 s incoherent integration. Fig. 6 shows the performance of the FENIX system with a GNSS-R system that obtains DDMs from GPS L1 C/A reflected signals. This system computes synthetic DDMswith an ad-hoc GNSS-R signal generator developed at UPC-CommSensLab with or without RFI signal. Fig. 6a shows the DDM with a very strong RFI signal that saturates the DDM computation and prevents observing the GPS reflected signal contribution. Conversely, Fig. 6b shows the DDM with the FENIX system activated. RFI-mitigated residuals can still be observed over the useful signal. However, the system can retrieve some geophysical parameters from the reflected GPS signal under RFI scenarios.

4. CONCLUSIONS

This new proposed architecture for the FENIX is proving to be an excellent solution to the RFI problem in a wide array of situations. With the addition of dual-band, automatic gain control and a new enclosure to survive the harshest conditions, this new version will become part of the state-of-the-art in highly RFI resilient GNSS-enabled applications. The new FPGA used in FENIX will provide the capability to evolve by using more advanced techniques or real-time reconfiguration to achieve optimal performance in a multitude of scenarios.

5. REFERENCES

[1] J. Querol Borràs, *Radio frequency interference detection and mitigation techniques for navigation and Earth observation*, Ph.D. thesis, Universitat Politècnica de Catalunya. Departament de Teoria del Senyal i Comunicacions, 2018, Available at: http://hdl.handle.net/2117/125028 Last visited: October 7, 2019.

[2] E. Kaplan and C. Hegarty, *Understanding GPS: Principles and Applications, Second Edition*, Artech House, 2005.

[3] R. D. De Roo, S. Misra, and C. S. Ruf, "Sensitivity of the Kurtosis Statistic as a Detector of Pulsed Sinusoidal RFI," *IEEE Transactions on Geoscience and Remote Sensing*, vol. 45, no. 7, pp. 1938–1946, jul 2007.

[4] J. M. Tarongi and A Camps, "Normality analysis for rfi detection in microwave radiometry," *Remote Sensing*, vol. 2, no. 1, pp. 191–210, 2010.

[5] D. G. Manolakis and V. K. Ingle, *Statistical and adaptive signal processing: spectral estimation, signal modeling, adaptive filtering, and array processing*, Artech House: signal processing library, 2000.

[6] J. Bartelt, N. Vucic, D. Camps-Mur, E. Garcia-Villegas, I. Demirkol, A. Fehske, M. Grieger, A. Tzanakaki, J. Gutiérrez, E. Grass, G. Lyberopoulos, and G. Fettweis, "5g transport network requirements for the next generation fronthaul interface," *EURASIP Journal on Wireless Communications and Networking*, vol. 2017, no. 1, pp. 89, May 2017.

[7] ETSI, *5G: Base Station (BS) radio transmission and reception*, October 2018, V15.3.0.

[8] Novatel, "GAJT-710ML Anti-Jam Antenna," Available at: `https://www.novatel.com/products/gnss-antennas/gajt-anti-jam-antennas/gajt/` Last visited: October 7, 2019.

[9] CESBIO, "RFI Monitoring," Available at: `http://www.cesbio.ups-tlse.fr/SMOS_blog/?page_id=4087` Last visited: October 7, 2019.